ISSN 0021-3640, JETP Letters, 2007, Vol. 85, No. 3, pp. 165–168. © Pleiades Publishing, Ltd., 2007.

Electronic Structure of α-Al_2O_3: Ab Initio Simulations and Comparison with Experiment¶

T. V. Perevalov[a], A. V. Shaposhnikov[a], V. A. Gritsenko[a, *], H. Wong[b], J. H. Han[c], and C. W. Kim[c]

[a] *Institute of Semiconductor Physics, Siberian Division, Russian Academy of Sciences, Novosibirsk, 630090 Russia*
** e-mail: grits@isp.ncs.ru*

[b] *Electronic Engineering Department, City University of Hong Kong, Tat Chee Avenue, Hong Kong, Korea*

[c] *Memory Division, Semiconductor Business, Samsung Electronics Co. Ltd., 449-711 San24, Nongseo-Dong, Kiheung-Gu, Yongin-City, Kyunggi-Do, Korea*

Received September 21, 2006; in final form, December 22, 2006

Al_2O_3 films 150 Å thick are deposited on silicon by the ALD technique, and their x-ray (XPS) and ultraviolet (UPS) photoelectron spectra of the valence band are investigated. The electronic band structure of corundum (α-Al_2O_3) is calculated by the ab initio density functional method and compared with the experimental results. The α-Al_2O_3 valence band consists of two subbands separated with an ionic gap. The lower band is mainly formed by oxygen 2*s* states. The upper band is formed by oxygen 2*p* states with a contribution of aluminum 3*s* and 3*p* states. A strong anisotropy of the effective mass is observed for holes: $m^*_{h\perp} \approx 6.3m_0$ and $m^*_{h\parallel} \approx 0.36m_0$. The effective electron mass is independent of the direction $m^*_{e\parallel} \approx m^*_{e\perp} \approx 0.4m_0$.

PACS numbers: 71.20.Ps, 72.80.Sk, 75.15.Mb, 77.84.Bw

DOI: 10.1134/S0021364007030071

Aluminum oxide Al_2O_3 is widely used as optical elements in lasers and optical devices, as a catalyst, and as a radiation-resistant transparent dielectric in nuclear power systems. Recently, Al_2O_3 thin films (≈50 Å) are intensively studied for their use in silicon devices as a gate dielectric in field-effect transistors and as a blocking layer in high-speed FLASH memory [1–3]. Al_2O_3 belongs to so-called high-k dielectrics possessing a high value of the dielectric constant (ϵ = 10) as compared to silicon oxide SiO_2 (ϵ), which is currently most widespread. The persistent trend toward a decrease in the channel length of silicon field-effect transistors requires a reduction in the effective thickness of gate SiO_2 to values <10 Å. In this case, the direct tunnel injection of electrons and holes through the dielectric becomes the main limiting factor. With the use of high-k dielectrics, the thickness of the gate-dielectric layer can be increased and spurious injection can be decreased. The injection of electrons and holes through a perfect (defectless) dielectric layer is performed by a tunneling mechanism. The rate of electron and hole injection exponentially depends on the electron m^*_e and hole m^*_h effective masses. The goal of this work is to experimentally and theoretically study the electronic structure of Al_2O_3 and to estimate the effective masses of electrons and holes.

In the crystalline state, aluminum oxide Al_2O_3 exists in the form of several allotropic modifications, corundum () being the most widespread and practically 1
important of them. The corundum crystal has hexagonal symmetry. The α-Al_2O_3 unit cell and the first Brillouin zone for a 30-atomic cell are shown in Figs. 1a and 1b. The hexagonal unit cell with parameters a = 4.76 Å and c = 12.99 Å containing 12 six-coordinated Al atoms and 18 four-coordinated O atoms [4] was used in the calculations [4] (see Table 1). The electronic structure of α-Al_2O_3 was studied experimentally by x-ray emission spectroscopy in [5]. Theoretically, the electronic structure of α-Al_2O_3 was studied in [6-9].

Al_2O_3 films 150 Å thick were deposited on silicon by atomic layer deposition (ALD) from trimethylaluminum $Al(CH_3)_3$. X-ray and ultraviolet photoelectron spectra (XPS and UPS, respectively) were measured on

Table 1. Position of basis atoms in α-Al_2O_3 (space group R–3cH) in the intrinsic (crystalline) coordinates

Atom	*x*	*y*	*z*
Al	0	0	0.35224
O	0.3065	0	0.25

¶ The text was submitted by the authors in English.

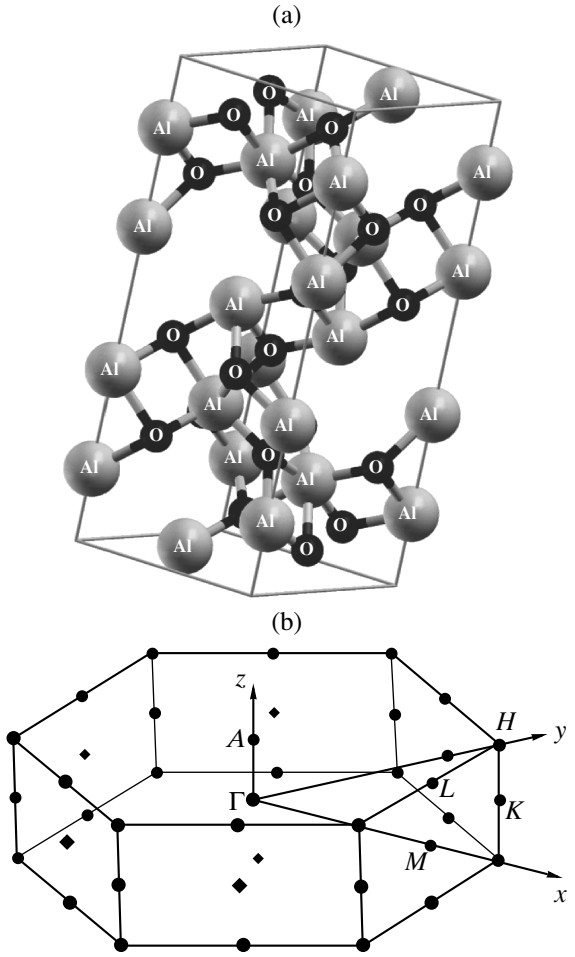

Fig. 1. (Upper panel) α-Al_2O_3 unit cell and (lower panel) the corresponding Brillouin zone with labeled symmetry points.

a Phi Quantum 2000 spectrometer. The XPS were excited by monochromated AlK_α radiation with the energy $\hbar\omega$ = 1486.6 eV. The UPS were excited by the HeII line of a helium lamp with the energy $\hbar\omega$ = 40.8 eV. The Al_2O_3 bandgap was determined by the electron energy loss technique using monochromatic electrons with an electron-beam energy of 200 eV on a LAS 3000 spectrometer.

The band structure calculations were performed using the Quantum-ESPRESSO program package [10]. The program is based on the density functional theory (DFT), a plane-wave basis set, and pseudopotentials for the description of core electrons. The periodic crystal structure is taken into account using periodic boundary conditions at the unit cell boundaries.

The following electronic configurations were used in the calculations: [Ne] $3s^23p^1$ for Al and [He] $2s^22p^4$ for O. The indicated states related to the valence shells, and [Ne] and [He] designated the core shells. The core electrons were described using the ultrasoft Vanderbilt pseudopotentials. The exchange–correlation functional

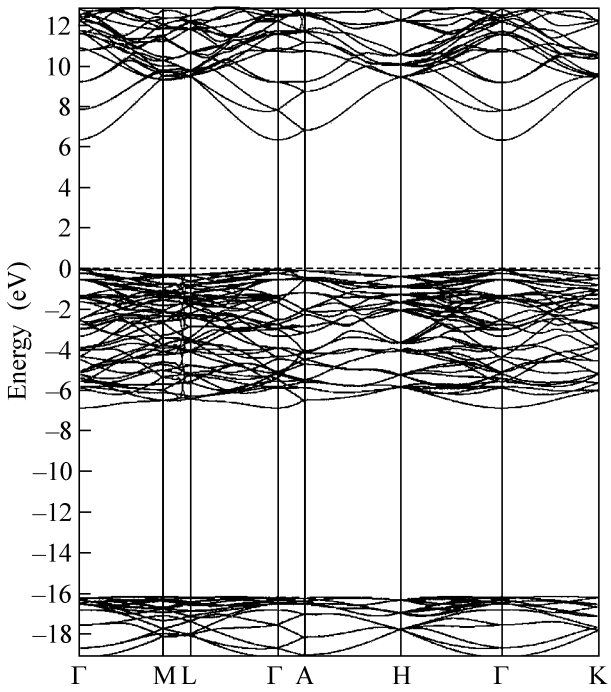

Fig. 2. α-Al_2O_3 band structure. The zero energy corresponds to the position of the valence band top.

was used in the local density approximation (LDA) with the PBE parameterization. The plane-wave cutoff energy in the self-consistent field (SCF) calculations was selected in such a way that the convergence in the total unit-cell energy be no worse than 0.001 Ry/atom and was taken equal to 55 Ry. The k-point mesh density in the reciprocal space was chosen based on the same considerations.

The effective electron and hole masses were numerically estimated by the obtained set of $E(k)$ points in the Brillouin zone by approximating the dispersion curve with a parabola in the vicinity of the local extremum. To accurately determine the positions of the extremal points (the valence band top and the conduction band bottom) and to obtain a dense point grid in the vicinity of extrema, additional non-SCF calculations were performed using the potentials obtained in the preceding SCF calculation.

Figure 2 presents the calculated band spectrum of α-Al_2O_3 electronic states. The calculated bandgap equals 6.26 eV. The ionic gap (the gap between the upper and lower valence bands) equals 8.9 eV.

The electron energy loss spectrum of Al_2O_3 at the energy of the monochromatic electron beam equal to 200 eV is presented in Fig. 3. The upper estimate for the bandgap width yields $E_g \le 8.8$ eV. This value is close to a value of 8.7 eV obtained from optical spectra in [11, 12]. The energy loss at 5.3 eV corresponds, presumably, to the excitation of defects in Al_2O_3. The measured energy of valence-electron plasma oscillations is $\hbar\omega_p$ =

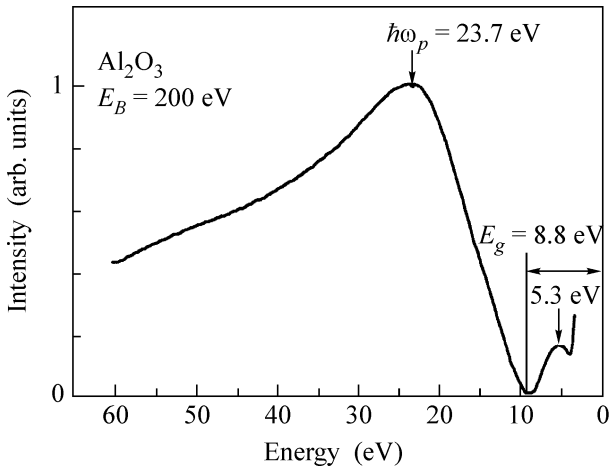

Fig. 3. Energy loss spectrum of monochromatic electrons. The incident beam energy is 200 eV. The zero energy corresponds to the energy of elastically scattered electrons.

23.7 eV. It is interesting to compare this value with the simple estimate for the free-electron gas, which is given by the equation

$$\omega_p^2 = 4\pi Ne^2/m.$$

Here, N is the concentration of valence electrons making a contribution to plasma oscillations. With regard to the O 2*p* and Al 3*s* and 3*p* valence electrons, this estimate gives the value $\hbar\omega_p = 24.2$ eV, which is close to an experimentally measured value of 23.7 eV. If it is assumed that the O 2*s* states (the lower valence band) also make a contribution to plasma oscillations, the calculated plasmon energy will be 27.9 eV, which is higher than the value observed experimentally.

The results of x-ray emission spectroscopy (taken from [5]), XPS, and UPS are presented in Fig. 4 on the same energy scale. The position of the valence band top (E_v) is taken as the zero energy. The experimental results are presented in solid lines, and the calculated partial densities of states with a given symmetry of wavefunctions are shown in dashed lines. The calculated spectra were broadened using a Lorentzian curve with a half-width of 0.25 eV. The fourth and sixth panels present the experimental UPS and XPS, respectively. Dashed lines present the calculated spectra obtained by summing the partial densities of states with regard to the corresponding photoionization cross sections taken from [13].

The valence band of Al_2O_3, like that of SiO_2, consists of two subbands separated with an ionic gap [14, 15]. The lower valence band (at an energy of ≈20 eV) is mainly formed by oxygen 2*s* orbitals with an admixture of aluminum 3*s* and 3*p* orbitals. The upper valence band (the energy in the range 0–12 eV in the experimental Si $L_{2,3}$ spectrum) is mainly formed by oxygen 2*p* and aluminum 3*s* and 3*p* orbitals. Note that the calculated relative intensities of peaks corresponding to

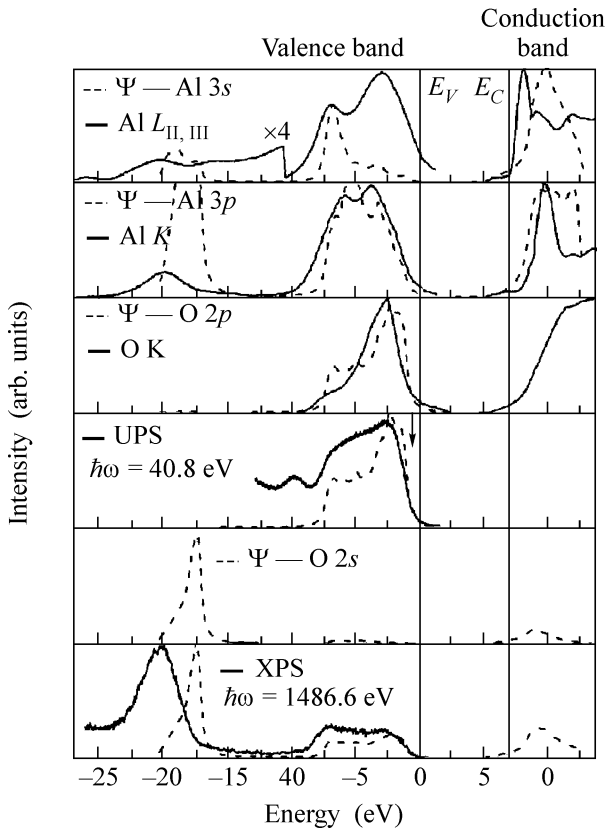

Fig. 4. Experimental data for (the first, second, and third panels from above) x-ray emission and absorption spectra taken from [5], (the fourth panel from above) ultraviolet photoelectron spectrum, and (the sixth panel from above) x-ray photoelectron spectrum. The zero energy (vertical line) corresponds to the position of the valence band top E_v. The conduction band bottom is denoted as E_c. Dashed lines designate theoretical densities of states in the valence and conduction bands. The symmetry of wavefunctions for electrons participating in x-ray transitions and the symmetry of wavefunctions for electrons related to partial densities of states are indicated in each panel.

the partial density of Al 3*p* states in the lower valence band substantially exceeds the intensities of peaks in the upper valence band. Previously, such a discrepancy for Si 3*p* peaks was observed in SiO_2 and Si_3N_4 [16, 17].

It should be noted that the features of the structure of the experimental Si $L_{2,3}$ spectrum cannot be adequately described using the calculated partial density of the Al 3*s* states. In particular, the upper peak at an energy of ≈–3 eV is absent in the Al 3*s* spectrum. In SiO_2 and Si_3N_4, where a similar discrepancy is observed, the upper peak in the valence band originates from silicon 3*d* orbitals and associated with nonlocal (two-center) transitions [16]. It is worth noting that, according to authors' calculations, the inclusion of silicon 3*d* orbitals does not lead to a significant change in the effective masses of electrons and holes in SiO_2 and Si_3N_4. The calculation of the Al_2O_3 band structure with

Table 2. Effective electron and hole masses in α-Al_2O_3 along the preferential directions in the Brillouin zone

Direction	m_h/m_0	m_e/m_0
Γ–M	6.2	0.39
Γ–A	0.36	0.41
Γ–K	6.4	0.39

a correct consideration of the contribution of aluminum 3*d* orbitals for the description of x-ray emission spectra was beyond the scope of this work. α-Al_2O_3 is a direct-gap dielectric whose valence band top and conduction band bottom are located at the center (Γ] point) of the Brillouin zone (Fig. 2). The calculated Al_2O_3 bandgap is 6.20 eV, which is lower than the experimental value $E_g \approx 8.7$ eV. This discrepancy is evidently associated with the fact that DFT systematically underestimate the bandgap width in solids.

Table 2 presents the calculated values of the electron and hole masses in α-Al_2O_3. The flat top of the valence band in the prism plane (Fig. 1) corresponds to heavy holes in the Γ–M, Γ–K direction. Light holes are observed in the perpendicular direction along the prism axis. It should be noted that the calculation gives two bands close in energy ($\Delta E \approx 0.01$ eV) at the valence band top (Γ point), which have an essentially different dispersion law. The band located lower corresponds to heavy holes with a mass tens of times higher.

The effective electron mass is in the range $m^*_{e\|} \approx m^*_{e\perp} \approx 0.4m_0$. This value should be compared with the experimental values of the tunneling effective mass for electrons in Al_2O_3 $m^*_e = (0.05–0.3)m_0$ [18], $m^*_e = 0.3m_0$ [19], and $m^*_e = (0.22–0.42)m_0$ [20]. It should be noted that an anisotropy of effective electron masses was found in [6], which is not confirmed in our work.

The calculations in this work were performed using the Quantum-EXPRESSO program package [10]. This work was supported by the Russian Foundation for Basic Research (project no. 06-02-16621), by the Siberian Division of the Russian Academy of Sciences (Integration Project no. 97), and by the Korean Ministry of Science and Technology (National Program of Tera-Level Nanodevices).

REFERENCES

1. A. I. Kingon, J. P. Maria, and S. K. Streiffer, Nature **406**, 1032 (2000).
2. G. D. Wilk, R. M. Wallace, and J. M. Anthony, J. Appl. Phys. **89**, 5243 (2001).
3. V. A. Gritsenko, K. A. Nasyrov, Yu. N. Novikov, et al., Solid-State Electron. **47**, 1651 (2003).
4. ICSD 2003 Collection, Entry # 88029.
5. I. A. Brytov and Yu. N. Romashchenko, Fiz. Tverd. Tela (Leningrad) **20**, 664 (1978) [Sov. Phys. Solid State **20**, 384 (1978)].
6. Y.-N. Xu and W. Y. Ching, Phys. Rev. B **43**, 4461 (1991).
7. K. Shiiki, M. Igorashi, and H. Kaijyu, Jpn. J. Appl. Phys., Part 1 **42**, 5185 (2003).
8. J. Robertson, J. Appl. Phys. **92**, 4712 (2002).
9. J. Robertson, Eur. Phys. J.: Appl. Phys. **28**, 265 (2004).
10. S. Baroni, A. Dal Corso, S. de Gironcoli, et al., http://www.pwscf.org/.
11. M. I. Boltz and R. H. French, Appl. Phys. Lett. **55**, 1955 (1989).
12. R. H. French, H. Mullejans, and D. J. Jones, J. Am. Ceram. Soc. **10**, 2549 (1998).
13. J.-J. Yeh, *Atomic Calculation of Photoionization Cross-Sections and Asymmetry Parameters* (Gordon and Breach, Amsterdam, 1993).
14. E. K. Chang, M. Rohlfing, and S. G. Louie, Phys. Rev. Lett. **85**, 2613 (2000).
15. Y.-N. Xu and W. Y. Ching, Phys. Rev. B **51**, 17 379 (1995).
16. V. A. Gritsenko, Yu. N. Novikov, A. V. Shaposhnikov, and Yu. N. Morokov, Fiz. Tekh. Poluprovodn. (St. Petersburg) **35**, 1041 (2001) [Semiconductors **35**, 997 (2001)].
17. V. A. Gritsenko, R. M. Ivanov, and Yu. N. Morokov, Zh. Éksp. Teor. Fiz. **108**, 2216 (1995) [JETP **81**, 1208 (1995)].
18. Z. Burstein and J. Levinson, Phys. Rev. B **12**, 3453 (1975).
19. Y.-C. Yeo, T.-J. King, and C. Hu, IEEE Trans. Electron Devices **50**, 1027 (2003).
20. A. Kerber, E. Cartier, R. Degraeve, et al., IEEE Trans. Electron Devices **50**, 1261 (2003).

Translated by A. Bagatur'yants

SPELL: 1. ()